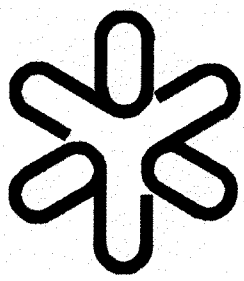

Instituto de Física
Universidade de São Paulo

Radion and Higgs Signals in Peripheral Heavy Ion Collisions at the LHC

S.M. Lietti[1] and C.G. Roldão[2]

1. Instituto de Física, Universidade de São Paulo, C.P. 66318, 05315-970, SP, Brasil

2. Instituto de Física Teórica, Universidade Estadual Paulista, Rua Pamplona 145, CEP1405-900, SP, Brasil

Publicação IF - 1548/2002

IFT–P.037/2002
IFUSP-1548/2002

Radion and Higgs Signals in Peripheral Heavy Ion Collisions at the LHC.

S. M. Lietti[1] and C. G. Roldão[2]
[1]*Instituto de Física da USP,*
C.P. 66.318, São Paulo, SP 05389-970, Brazil.
[2]*Instituto de Física Teórica, Universidade Estadual Paulista,*
Rua Pamplona 145, CEP 01405-900 São Paulo, Brazil.
(May 22, 2002)

Abstract

We investigate the sensitivity of the heavy ion mode of the LHC to Higgs boson and Radion production via photon-photon fusion through the analysis of the processes $\gamma\gamma \to \gamma\gamma$, $\gamma\gamma \to b\bar{b}$, and $\gamma\gamma \to gg$ in peripheral heavy ion collisions. We suggest cuts to improve the Higgs and Radion signal over standard model background ratio and determine the capability of LHC to detect these particles production.

I. INTRODUCTION

The standard model (SM) has been very successful in accounting for almost all experimental data. The Higgs boson is the only particle in the SM that has not yet been confirmed experimentally. It is responsible for the mass generation of fermions and gauge bosons. The search for the Higgs boson is the main priority in high energy experiments and hints of its existence may have been already seen at LEP [1] at around $m_H \sim 115$ GeV. Nevertheless, the SM can only be a low energy limit of a more fundamental theory because it cannot explain a number of theoretical issues, one of which is the gauge hierarchy problem between the only two known scales in particle physics – the weak and Planck scales. Recent advances in string theories have revolutionized our perspectives and understanding of the problems, namely, the Planck, grand unification, and string scales can be brought down to a TeV range with the help of extra dimensions, compactified or not. Arkani-Hamed *et al.* [2] proposed that using compactified dimensions of large size (as large as mm) can bring the Planck scale down to TeV range. Randall and Sundrum [3] proposed a 5-dimensional space-time model with a nonfactorizable metric to solve the hierarchy problem. The Randall-Sundrum model (RSM) has a four-dimensional massless scalar, the modulus or Radion. The most important ingredients of the above model are the required size of the Radion field such that it generates the desired weak scale from the scale M ($\approx$ Planck scale) and the stabilization of the Radion field at this value. A stabilization mechanism was proposed by Goldberger and Wise [4].

As a consequence of this stabilization, the mass of the Radion is of order of O(TeV) and the strength of coupling to the SM fields is of order of $O(1/\text{TeV})$. Therefore, the detection of this Radion will be the first signature of the RSM and the stabilization mechanism by Goldberger and Wise.

Higgs and Radion can be produced in various types of accelerators. Several papers have been published in order to study the possibility of detection of the Higgs particle in e^+e^-, $\mu^+\mu^-$, $p\bar{p}$, pp and $\gamma\gamma$ colliders [5]. Recently, the phenomenology of the Radion particle has been also studied for e^+e^-, pp and $\gamma\gamma$ colliders [6]. In this paper we explore the possibility of an intermediate-mass Higgs boson or Radion scalar be produced in peripheral heavy ion collisions through photon-photon interactions [7,8]. The reason to choose photon-photon fusion in peripheral heavy ion collisions resides in the fact that the production mode is free of any problem caused by strong interactions of the initial state, which make these processes cleaner than pomeron-pomeron or pomeron-photon fusions. In the context of the SM, the Higgs boson has been explored in detail in the literature [9,10], with the general conclusion that the chances of finding the SM Higgs in the photon-photon case are marginal. On the other hand, a study of Radion production in peripheral heavy ion collisions has not yet been made.

The Higgs couplings considered in this paper are given by the usual SM lagrangian while the Radion effects can be described by effective operators involving the spectrum of the SM and the Radion scalar field. The Radion couplings to the SM particles are similar to the Higgs couplings to the same particles, except from a factor involving the Higgs and the Radion vacuum expectation values (vev's), as can be seen in Section II. In Section III we present the strategy to evaluate photon-photon fusion processes in peripheral heavy ion collisions and in Section IV we explore the capabilities of peripheral heavy ion collisions in detecting Higgs and Radion productions by analyzing the processes $\gamma\gamma \to \gamma\gamma$, $b\bar{b}$, and gg. After simulating the signal and background, we find optimal cuts to maximize their ratio. We show how to use the invariant mass spectra of the final state $\gamma\gamma$, $b\bar{b}$, and gg pairs in order to improve the SM Higgs boson and RMS Radion signals. Finally, in Section V we draw our final conclusions.

II. EFFECTIVE LAGRANGIAN FOR THE RADION COUPLINGS

In order to describe the interactions of the RSM Radion with the SM particles, we follow the notation of Ref. [6]. These interactions are model-independent and are governed by 4-dimensional general covariance, and thus given by the following Lagrangian

$$\mathcal{L}_{\text{int}} = \frac{R}{\Lambda_R} T^{\mu}_{\mu}(\text{SM}) \,, \tag{1}$$

where $\Lambda_R = \langle R \rangle$ is of order TeV, and T^{μ}_{μ} is the trace of SM energy-momentum tensor, which is given by

$$T^{\mu}_{\mu}(\text{SM}) = \sum_f m_f \bar{f} f - 2m_W^2 W^+_\mu W^{-\mu} - m_Z^2 Z_\mu Z^\mu + (2m_H^2 H^2 - \partial_\mu H \partial^\mu H) + \ldots \,, \tag{2}$$

where ... denotes higher order terms. The couplings of the Radion with fermions and W, Z and Higgs bosons are given in Eq. (1). Note that the couplings of the Radion with fermions,

W, and Z are similar to the couplings of the Higgs to these particles, the only difference resides in the coupling constants where v, the vev of the Higgs field, is replaced by Λ_R.

The coupling of the Radion to a pair of gluons (photons) is given by contributions from 1-loop diagrams with the top-quark (top-quark and W) in the loop, similar to the Higgs boson couplings to the same pair. However, for the Radion case, there is another contribution coming from the trace anomaly for gauge fields, that is given by

$$T^{\mu}_{\mu}(\mathrm{SM})^{\mathrm{anom}} = \sum_a \frac{\beta_a(g_a)}{2g_a} F^a_{\mu\nu} F^{a\mu\nu} \,. \tag{3}$$

For the coupling of the Radion to a pair of gluons, $\beta_{\mathrm{QCD}}/2g_s = -(\alpha_s/8\pi)b_{\mathrm{QCD}}$, where $b_{\mathrm{QCD}} = 11 - 2n_f/3$ with $n_f = 6$. Thus, the effective coupling of $Rg(p_{1,\mu,a})g(p_{2,\nu,b})$, including the 1-loop diagrams of top-quark and the trace anomaly contributions is given by

$$\frac{i\delta_{ab}\alpha_s}{2\pi\Lambda_R}\left[b_{\mathrm{QCD}} + y_t(1+(1-y_t)f(y_t))\right]\left(p_1\cdot p_2 g_{\mu\nu} - p_{2_\mu}p_{1_\nu}\right) \,, \tag{4}$$

where $y_t = 4m_t^2/2p_1\cdot p_2$.

The effective coupling of $R\gamma(p_{1,\mu})\gamma(p_{2,\nu})$, including the 1-loop diagrams of the top-quark and W boson, and the trace anomaly contributions is given by

$$\frac{i\alpha_{\mathrm{em}}}{2\pi\Lambda_R}\left[b_2 + b_Y - (2+3y_W+3y_W(2-y_W)f(y_W)) + \frac{8}{3}y_t(1+(1-y_t)f(y_t))\right] \times \left(p_1\cdot p_2 g_{\mu\nu} - p_{2_\mu}p_{1_\nu}\right) \,, \tag{5}$$

where $y_i = 4m_i^2/2p_1\cdot p_2$, $b_2 = 19/6$ and $b_Y = -41/6$. In the above, the function $f(z)$ is given by

$$f(z) = \begin{cases} \left[\sin^{-1}\left(\frac{1}{\sqrt{z}}\right)\right]^2 \,, & z \geq 1 \\ -\frac{1}{4}\left[\log\frac{1+\sqrt{1-z}}{1-\sqrt{1-z}} - i\pi\right]^2 \,, & z < 1 \end{cases} \,.$$

Equations (1–5) give all necessary couplings to perform calculations on decays and production of the Radion. In order to perform calculations on the decays and production of the Higgs, we consider its SM couplings, widely discussed in the literature.

III. SIMULATIONS

In order to perform the Monte Carlo analysis, we have employed the package MadGraph [11] coupled to HELAS [12]. Special subroutines were constructed for the anomalous contribution which enable us to take into account all interference effects between the QED and the anomalous amplitudes. The phase space integration was performed by VEGAS [13].

The photon distribution in the nucleus can be described using the equivalent-photon or Weizsäcker-Williams approximation in the impact parameter space. Denoting the photon distribution function in a nucleus by $F(x)$, which represents the number of photons carrying a fraction between x and $x+dx$ of the total momentum of a nucleus of charge Ze, we can define the two-photon luminosity through

$$\frac{dL}{d\tau} = \int_{\tau}^{1} \frac{dx}{x} F(x)F(\tau/x), \tag{6}$$

where $\tau = \hat{s}/s$, $\hat{s}$ is the square of the center of mass (c.m.s.) system energy of the two photons and s of the ion-ion system. The total cross section $AA \to AA\gamma\gamma \to AAX$, where X are the particles produced by the $\gamma\gamma$ process, is

$$\sigma(s) = \int d\tau \frac{dL}{d\tau} \hat{\sigma}(\hat{s}), \tag{7}$$

where $\hat{\sigma}(\hat{s})$ is the cross-section of the subprocess $\gamma\gamma \to X$.

We choose to use the conservative and more realistic photon distribution of Cahn and Jackson [10], including a prescription proposed by Baur [8] for realistic peripheral collisions, where we must enforce that the minimum impact parameter (b_{min}) should be larger than $R_1 + R_2$, where R_i is the nuclear radius of the ion i. A useful fit for the two-photon luminosity is:

$$\frac{dL}{d\tau} = \left(\frac{Z^2\alpha}{\pi}\right)^2 \frac{16}{3\tau} \xi(z), \tag{8}$$

where $z = 2MR\sqrt{\tau}$, M is the nucleus mass, R its radius and $\xi(z)$ is given by

$$\xi(z) = \sum_{i=1}^{3} A_i e^{-b_i z}, \tag{9}$$

which is a fit resulting from the numerical integration of the photon distribution, accurate to 2% or better for $0.05 < z < 5.0$, and where $A_1 = 1.909$, $A_2 = 12.35$, $A_3 = 46.28$, $b_1 = 2.566$, $b_2 = 4.948$, and $b_3 = 15.21$. For $z < 0.05$ we use the expression (see Ref. [10])

$$\frac{dL}{d\tau} = \left(\frac{Z^2\alpha}{\pi}\right)^2 \frac{16}{3\tau} \left[\ln\left(\frac{1.234}{z}\right)\right]^3. \tag{10}$$

In this paper we consider electromagnetic processes of peripheral Ar-Ar and Pb-Pb collisions in order to produce a Higgs and/or Radion scalar via photon-photon fusion since the pomeron contributions are negligible for subprocesses with center of mass energy close to the Higgs mass. According to Ref. [14], the total center of mass energy for $^{40}_{18}$Ar ($^{208}_{82}$Pb) is equal to 7 (5.5) TeV/nucleon and an average luminosity of $5.2 \times 10^{29} (4.2 \times 10^{26})$ cm^{-2} s^{-1}, which implies an effective photon-photon luminosity for $m_{\gamma\gamma} = 115$ GeV equals to $2 \times 10^{28} (8 \times 10^{26})$ cm^{-2} s^{-1} [0.63 (0.0025) pbarn^{-1} year^{-1}] at LHC, as can be seen in Figure 1, which was extracted from Ref. [14]. We will also consider the optimistic possibility of Ca-Ca collisions [15,16], where the total center of mass energy for $^{40}_{20}$Ca is equal to 7 TeV/nucleon and an average luminosity of 5×10^{30} cm^{-2} s^{-1}, which implies an effective photon-photon luminosity for $m_{\gamma\gamma} = 115$ GeV equals to 1.92×10^{29} cm^{-2} s^{-1} (6 pbarn^{-1} year^{-1}).

IV. RESULTS

In our analyses, we computed the cross sections for the Higgs and Radion production via photon-photon fusion in peripheral heavy ion collisions at LHC, with the subsequent decay

of the Higgs and/or Radion into $\gamma\gamma$, $b\bar{b}$ and gg pairs. The main sources of background for these processes are the box diagram for the process $\gamma\gamma \to \gamma\gamma$, the usual electromagnetic tree level diagrams for the process $\gamma\gamma \to b\bar{b}$, and the box diagram $\gamma\gamma \to gg$ and the usual tree level diagrams $\gamma\gamma \to q\bar{q}$, where $q = u, d, s, c$, for the process $\gamma\gamma \to gg$.

We begin our analyses using similar cuts and efficiencies as the ones ATLAS Collaboration [17] applied in their studies of Higgs boson searches. Our initial results are obtained imposing the following acceptance set of cuts:

$$p_T^{\gamma(b)[g]} > 25 \text{ GeV} \quad , \qquad |\eta_{\gamma(b)[g]}| < 2.5 \quad , \qquad \Delta R_{\gamma\gamma(b\bar{b})[\bar{g}g]} > 0.4 \ , \tag{11}$$

and taking into account an efficiency for reconstruction and identification of one photon of 84%, an efficiency of reconstruction for $H \to b\bar{b}$ of 90% with a b-tagging of 60% per each quark b [17], and finally an efficiency of reconstruction for $H \to q\bar{q}$ or gg of 80%. Taking all these efficiencies into account, the cross sections are evaluated with a total efficiency factor of 70(32)[80]% for the decay H or $R \to \gamma\gamma(b\bar{b})[gg]$. The results are presented in Table I for a Higgs and Radion masses of 115 GeV, with $\Lambda_R = 4v \approx 1$ TeV, in peripheral Ar-Ar and Pb-Pb collisions at LHC. Results for Ca-Ca collisions at LHC can also be obtained, according to Equation (8), by simply multiplying the results for Ar-Ar collisions by the factor $(\frac{Z_{Ca}}{Z_{Ar}})^4 = (\frac{20}{18})^4 \approx 1.524$.

In order to improve the Higgs and Radion signal over SM background, i.e., all other Feynman diagrams that contribute to the process considered, we have studied several kinematical distributions of the final state particles. Since the Higgs and Radion interactions occur mainly when these particles are produced on-shell, the most promising one is the invariant mass of the final particles.

The behavior of the normalized invariant mass distribution of the final state particles is plotted in Figure 2 for the process $\gamma\gamma \to b\bar{b}$ with a Higgs mass and a Radion mass equal to 115 GeV and $\lambda_R = 4v \approx 1$ TeV. For instance, if we impose an additional cut of $|m_{b\bar{b}} - m_H| < 15$ GeV in the process $\gamma\gamma \to b\bar{b}$, the value for the SM background cross section in peripheral Ar-Ar collisions is reduced from 6.927 pb to 0.8486 pb, while the value for the Higgs (Radion) cross section ($\gamma\gamma \to H(R) \to b\bar{b}$) is almost unaffected, varying from $0.1038(1.923\times10^{-2})$ pb to $0.1038(1.919\times10^{-2})$ pb when the invariant mass cut is imposed. Similar behavior is observed in the processes $\gamma\gamma \to \gamma\gamma$ and $\gamma\gamma \to gg$, as can be seen in Table II. Therefore we collected final states $\gamma\gamma$, $b\bar{b}$ and gg events whose invariant masses fall in bins of size of 30 GeV around the Higgs (Radion) mass

$$m_{H(R)} - 15 \text{ GeV} < m_{\gamma\gamma(b\bar{b})[gg]} < m_{H(R)} + 15 \text{ GeV} \tag{12}$$

in order to evaluate our results.

Considering the effective photon-photon luminosities given by Figure 1 and Refs. [14,15], we note that the Ar-Ar(Ca-Ca) luminosity is $\approx$250(2500) times greater than the Pb-Pb luminosity. On the other hand, Table II shows that the Pb-Pb cross sections are $\approx$30(20) times greater than the Ar-Ar(Ca-Ca) cross sections. Taking into account both luminosity and cross section behavior for each mode of the heavy ion LHC accelerator, one can realize that the total number of events in Ar-Ar(Ca-Ca) collisions is $\approx$8(125) times greater than in Pb-Pb collisions, which shows that Pb-Pb collisions is less indicated than Ar-Ar(Ca-Ca) collisions for photon-photon fusion processes with a typical center of mass energy of $\mathcal{O}(100)$ GeV. Therefore, the Pb-Pb mode will not be considered form this point on in our analysis.

Another information that can be extracted from Figure 1 is the dependence between the effective photon-photon luminosity and the invariant mass of the initial $\gamma\gamma$ pair, which indicates that a discovery of a SM Higgs or a RSM Radion production via photon-photon fusion is favored for low values for the invariant mass of the initial $\gamma\gamma$ pair. Similar conclusion can be obtained from Figure 3, where the behavior of the cross sections of the processes $\gamma\gamma \to \gamma\gamma$, $\gamma\gamma \to b\bar{b}$, and $\gamma\gamma \to gg$, for events whose invariant masses fall in bins of size of 30 GeV around the mass M used to impose the cut in Equation (12), is presented for $\lambda_R = 4v \approx 1$ TeV. Higher values for the cross sections are obtained for masses M lower than 200 GeV. Therefore, from this point on, we will only consider in our analysis a SM Higgs and a RSM Radion mass of 115 GeV, as indicated by the latest hints from the LEP Higgs search [1] experiment.

Another point considered in our analyses is the dependence between the cross sections for the Radion contribution of the three processes and the ratio of the vev's of the Radion (Λ_R) and the Higgs (v) fields. Figure 4 shows the behavior of the cross sections in the range $0.5 \leq \frac{\Lambda_R}{v} \leq 4$. Note that Figures 4 (a) and (b) show that the SM Higgs contribution is greater than the RSM Radion contribution in the processes $\gamma\gamma \to \gamma\gamma$ and $\gamma\gamma \to b\bar{b}$, while Figure 4 (c) shows that the RSM Radion contribution is greater than the SM Higgs contribution in the process $\gamma\gamma \to gg$. Therefore, the process $\gamma\gamma \to gg$ is the most sensitive for a Radion search while the other two processes are most sensitive for a Higgs search.

In order to identify a 95% C.L. signal of a SM Higgs or a RSM Radion production at the heavy ion mode of the LHC, let us consider the significance (S) of a signal given by the equation

$$S = \frac{N_{Total} - N_{Background}}{\sqrt{N_{Total}}} = \frac{\sigma_{Total} - \sigma_{Background}}{\sqrt{\sigma_{Total}}}\sqrt{\mathcal{L}}, \tag{13}$$

where N is the number of events, $\mathcal{L}$ is the integrated luminosity of the accelerator, σ is cross section of the process considered. The subscript *Background* stands for the SM background contribution without any Higgs and/or Radion diagrams, and the subscript *Total* stands for the total contribution, including Higgs and/or Radion diagrams. A 95% C.L. signal is obtained when $S = 1.96$ for Gaussian distributions. The results presented in Table II for the ${}^{40}_{18}$Ar mode show that the SM background cross sections are at least one order of magnitude higher than the Higgs or Radion signals. Note that if one has one event identified as a Higgs or Radion exchange, than there will be at least ten SM background events, fact that justifies a Gaussian distribution approach.

Therefore, it is possible to evaluate the integrated luminosity needed for a 95% C.L. Higgs signal by taking in Equation (13) $S = 1.96$ and the cross sections presented in Table II, with σ_{Total} given by the sum $(\sigma_{Background} + \sigma_{Higgs})$ since the interference effects are negligible, as checked in our MadGraph/Helas code. The results are presented in Table III, where the number of years needed to establish a 95% C.L. Higgs signal is also shown when we consider the accelerator luminosity given by $\mathcal{L} = 0.63$ pb^{-1} year^{-1}, as discussed above in the text. Table III also shows the results for the Ca-Ca mode of the accelerator, with luminosity given by $\mathcal{L} = 6$ pb^{-1} year^{-1}. Analogously, a 95% C.L. Higgs plus Radion signal can be considered by simply taking $\sigma_{Total} = (\sigma_{Background} + \sigma_{Higgs} + \sigma_{Radion})$, and the results for this case is presented in Table IV.

The results in Table III indicate that the process $\gamma\gamma \to b\bar{b}$ is the best choice to search the Higgs boson because the integrated luminosity needed for a 95% C.L. signal (≈ 250 pb^{-1})

is three orders of magnitude smaller than the luminosity needed for the process $\gamma\gamma \to \gamma\gamma$ and five orders of magnitude smaller than the luminosity needed for the process $\gamma\gamma \to gg$. However, this integrated luminosity is still very high compared to the luminosity expected for both Ar-Ar and Ca-Ca mode, tens of years being needed for a 95% C.L. signal detection.

The results in Table IV include the RMS Radion in the analysis. There are small changes for the $\gamma\gamma \to b\bar{b}$ and $\gamma\gamma \to \gamma\gamma$ processes. The main difference appears in the $\gamma\gamma \to gg$ process, where the integrated luminosity needed for a 95% C.L. signal is three orders of magnitude smaller than the one of Table III. The reason for this change is that the Radion contribution is greater than the Higgs contribution only in the process $\gamma\gamma \to gg$, as can be seen in Figs. 3(c) and 4(c).

In order to improve the results, one could collected final states $\gamma\gamma$, $b\bar{b}$ and gg events whose invariant masses fall in bins of size of 10 GeV around the Higgs (Radion) mass

$$m_{H(R)} - 5 \text{ GeV} < m_{\gamma\gamma(b\bar{b})[gg]} < m_{H(R)} + 5 \text{ GeV}. \tag{14}$$

In this situation, the SM background is even more reduced while the Higgs and Radion signals are unchanged, as can be seen in Table V. The total integrated luminosity needed for a 95% C.L. Higgs (Higgs plus Radion) signal are now presented in Table VI (VII).

The number of years needed for a 95% C. L. Higgs signal in the process $\gamma\gamma \to b\bar{b}$ at the Ca-Ca mode of the accelerator is reduced to $\approx$ 15 years. When the Radion is included in the analysis, the number of years is reduced to $\approx$ 12.5 years. If the experiment luminosity could be enhanced by a factor of ten, then a 95% C. L. SM Higgs signal could be obtained in 18 months. Still in this case, if a 95% C. L. signal were obtained in 15 months, it would be an indication of the existence of the RMS Radion. If the experiment luminosity could be enhanced by a factor of twenty, then a 95% C. L. RMS Radion signal in the process $\gamma\gamma \to gg$ could be obtained in 31 months.

V. CONCLUSIONS

In this work we have studied the sensitivity of the heavy ion mode of the LHC to detect the production of Higgs and Radion scalars via photon-photon fusion through the analysis of the processes $\gamma\gamma \to \gamma\gamma, b\bar{b}$ and gg in peripheral heavy ion collisions.

The chances of finding the SM Higgs boson (or the RMS Radion) are marginal for high values of the Higgs (Radion) mass. For lower masses the situation is still critical, but there is some hope left. We have considered $M_H = M_R = 115$ GeV in our analysis according to the recent LEP hints on the Higgs mass.

The best place to search the Higgs boson is in the Ca-Ca ion mode of the LHC accelerator through the analysis of the process $\gamma\gamma \to b\bar{b}$. In this case, considering the luminosities presented in the literature, a 95% C. L. signal can be established in 15 years of run. If the Radion scalar of the RSM is taken into account, a 95% C. L. signal would be established in 12.5 years. If the experiments could enhance their expectation for the luminosity by a factor of 10, then a 95% C. L. SM Higgs signal could be established in less than two years of run.

On the other hand, the best place to search the Radion of the RSM is in the Ca-Ca ion mode of the LHC accelerator through the analysis of the process $\gamma\gamma \to gg$. In this case,

the experiments would have to improve their luminosity prediction by a factor of twenty in order to establish a 95% C. L. Radion signal in less than three years of run.

In conclusion, SM Higgs and RMS Radion observation in the heavy ion mode of the LHC accelerator is improbable, unless the expected luminosity of the experiment could be enhanced by a factor of 10–20.

ACKNOWLEDGMENTS

S. M. L. wishes to thank O. J. P. Éboli for encouragement and C. G. R. wishes to thank S. Klein for useful discussions. This work was supported by Fundação de Amparo à Pesquisa do Estado de São Paulo (FAPESP).

REFERENCES

[1] See `http://delphiwww.cern.ch/~offline/physics_links/lepc.html`.

[2] N. Arkani-Hamed, S. Dimopoulos, and G. Dvali, Phys. Lett. **B429**, 263 (1998); I. Antoniadis *et al.*, Phys. Lett. **B436**, 257 (1998).

[3] L. Randall and R. Sundrum, Phys. Rev. Lett. **83**, 3370 (1999); *ibid.* **83**, 4690 (1999).

[4] W. Goldberger and M. Wise, Phys. Rev. Lett. **83**, 4922 (1999); W. Goldberger and M. Wise, Phys. Lett. **B475**, 275 (2000).

[5] A. Sopczak, "Complete LEP data: Status of Higgs boson searches," hep-ph/0112082; M. S. Berger, "Higgs bosons at muon colliders," in *Proc. of the APS/DPF/DPB Summer Study on the Future of Particle Physics (Snowmass 2001)* ed. R. Davidson and C. Quigg, hep-ph/0110390; M. Carena *et al.*, "Report of the Tevatron Higgs working group," hep-ph/0010338; D. Zeppenfeld, "Higgs Physics At The Lhc," Int. J. Mod. Phys. A **16S1B**, 831 (2001); D. M. Asner, J. B. Gronberg and J. F. Gunion, "Detecting and studying Higgs bosons in two-photon collisions at a linear collider," hep-ph/0110320.

[6] K. Cheung, Phys. Rev. D **63**, 056007 (2001).

[7] G. Baur, J. Phys. **G24** (1998) 1657 .

[8] G. Baur, K. Hencken and D. Trautmann, hep-ph/9810418; C. A. Bertulani and G. Baur, Phys. Reports **163** (1988) 299 ; G. Baur, in *Proceedings of the CBPF International Workshop on Relativistic Aspects of Nuclear Physics*, Rio de Janeiro, 1989, edited by T. Kodama *et al.* (World Scientific, Singapore, 1990), p. 127; G. Baur and C. A. Bertulani, Nucl. Phys. **A505** (1989) 835.

[9] E. Papageorgiu, Phys. Rev. **D40** (1989) 92; Nucl. Phys. **A498** (1989) 593c; M. Grabiak *et al.*, J. Phys. **G15** (1989) L25; M. Drees, J. Ellis and D. Zeppenfeld, Phys. Lett. **B223** (1989) 454; M. Greiner, M. Vidovic, J. Rau and G. Soff, J. Phys. **G17** (1991) L45; B. Müller and A. J. Schramm, Phys. Rev. **D42** (1990) 3699; B. Müller and A. J. Schramm, Nucl. Phys. **A523** (1991) 677; J. S. Wu, C. Bottcher, M. R. Strayer, and A. K. Kerman, Ann. Phys. **210** (1991) 402.

[10] R. N. Cahn and J. D. Jackson, Phys. Rev. **D42** (1990) 3690.

[11] T. Stelzer and W. F. Long, Comput. Phys. Commun. **81** (1994) 357.

[12] H. Murayama, I. Watanabe and K. Hagiwara, KEK Report 91-11 (unpublished).

[13] G. P. Lepage, J. Comp. Phys. **27** (1978) 192, and "Vegas: An Adaptive Multidimensional Integration Program", CLNS-80/447, 1980 (unpublished).

[14] G. Baur, K. Hencken, D. Trautmann, S. Sadovsky and Y. Kharlov, hep-ph/0112211.

[15] E. Papageorgiu, "Searching for an intermediate-mass Higgs and new physics in two-photon coherent processes at the LHC," hep-ph/9507221.

[16] S. M. Lietti, A. A. Natale, C. G. Roldao and R. Rosenfeld, Phys. Lett. B **497** (2001) 243.

[17] Atlas Detector and Physics Performance Technical Design Report, `http://press.web.cern.ch/Atlas/GROUPS/PHYSICS/TDR/access.html`.

TABLES

Ion considered	Final State	$\sigma_{Background}$ (pb)	σ_{Higgs} (pb)	σ_{Radion} (pb)
$^{40}_{18}$Ar	$\gamma\gamma$	1.961×10^{-2}	1.346×10^{-4}	3.020×10^{-5}
$^{40}_{18}$Ar	$b\bar{b}$	6.927×10^{0}	1.038×10^{-1}	8.982×10^{-3}
$^{40}_{18}$Ar	gg	5.682×10^{2}	2.874×10^{-3}	1.334×10^{-1}
$^{208}_{82}$Pb	$\gamma\gamma$	1.160×10^{0}	3.913×10^{-3}	8.627×10^{-4}
$^{208}_{82}$Pb	$b\bar{b}$	3.919×10^{2}	3.023×10^{0}	2.666×10^{-1}
$^{208}_{82}$Pb	gg	3.179×10^{4}	8.344×10^{-2}	3.883×10^{0}

TABLE I. Cross Section in pb for the process $\gamma\gamma \to$ Final State with $m_H = m_R = 115$ GeV and $\Lambda_R = 4v = 984$ GeV ≈ 1 TeV in heavy ion collisions at LHC with the acceptance set of cuts of Equation (11). $\sigma_{Background}$ stands for the SM background, σ_{Higgs} stands for the contribution $\gamma\gamma \to H \to$ Final State and σ_{Radion} stands for the contribution $\gamma\gamma \to R \to$ Final State.

Ion considered	Final State	$\sigma_{Background}$ (pb)	σ_{Higgs} (pb)	σ_{Radion} (pb)
$^{40}_{18}$Ar	$\gamma\gamma$	2.050×10^{-3}	1.349×10^{-4}	3.030×10^{-5}
$^{40}_{18}$Ar	$b\bar{b}$	8.486×10^{-1}	1.038×10^{-1}	9.254×10^{-3}
$^{40}_{18}$Ar	gg	7.170×10^{1}	2.875×10^{-3}	1.338×10^{-1}
$^{208}_{82}$Pb	$\gamma\gamma$	6.589×10^{-2}	4.103×10^{-3}	9.222×10^{-4}
$^{208}_{82}$Pb	$b\bar{b}$	2.721×10^{1}	3.159×10^{0}	2.818×10^{-1}
$^{208}_{82}$Pb	gg	2.298×10^{3}	8.753×10^{-2}	4.072×10^{0}

TABLE II. Cross Section in pb for the process $\gamma\gamma \to$ Final State with $m_H = m_R = 115$ GeV and $\Lambda_R = 4v = 984$ GeV ≈ 1 TeV in heavy ion collisions at LHC with the refined set of cuts of Equations (11) and (12). $\sigma_{Background}$ stands for the SM background without Higgs and/or Radion diagrams, σ_{Higgs} stands for the contribution $\gamma\gamma \to H \to$ Final State and σ_{Radion} stands for the contribution $\gamma\gamma \to R \to$ Final State.

Ion considered	Final State	Integrated Luminosity (pb^{-1})	Years
$^{40}_{18}$Ar	$\gamma\gamma$	4.612×10^{5}	7.321×10^{5}
$^{40}_{18}$Ar	$b\bar{b}$	3.396×10^{2}	5.390×10^{2}
$^{40}_{18}$Ar	gg	3.333×10^{7}	5.290×10^{7}
$^{40}_{20}$Ca	$\gamma\gamma$	3.026×10^{5}	5.044×10^{4}
$^{40}_{20}$Ca	$b\bar{b}$	2.228×10^{2}	3.713×10^{1}
$^{40}_{20}$Ca	gg	2.186×10^{7}	3.644×10^{6}

TABLE III. Total Integrated Luminosity needed for a 95% C.L. Higgs signal for the process $\gamma\gamma \to$ Final State with $m_H = 115$ GeV in heavy ion collisions at LHC with the refined set of cuts of Equations (11) and (12). It is also presented the number of years needed for a 95% C.L. Higgs signal considering a luminosity of $0.63(6)\text{pb}^{-1}$ year^{-1} for the Ar-Ar (Ca-Ca) mode as discussed in the text.

Ion considered	Final State	Integrated Luminosity (pb^{-1})	Years
$^{40}_{18}Ar$	$\gamma\gamma$	3.118×10^{5}	4.950×10^{5}
$^{40}_{18}Ar$	$b\bar{b}$	2.890×10^{2}	4.588×10^{2}
$^{40}_{18}Ar$	gg	1.477×10^{4}	2.345×10^{4}
$^{40}_{20}Ca$	$\gamma\gamma$	2.046×10^{5}	3.410×10^{4}
$^{40}_{20}Ca$	$b\bar{b}$	1.896×10^{2}	3.161×10^{1}
$^{40}_{20}Ca$	gg	9.693×10^{3}	1.615×10^{3}

TABLE IV. Total Integrated Luminosity needed for a 95% C.L. Higgs plus Radion signal for the process $\gamma\gamma \to$ Final State with $m_H = m_R = 115$ GeV and $\Lambda_R = 4v = 984$ GeV ≈ 1 TeV in heavy ion collisions at LHC with the refined set of cuts of Equations (11) and (12). It is also presented the number of years needed for a 95% C.L. Higgs plus Radion signal considering a luminosity of $0.63(6)pb^{-1}$ $year^{-1}$ for the Ar-Ar (Ca-Ca) mode as discussed in the text.

Ion considered	Final State	$\sigma_{Background}$ (pb)	σ_{Higgs} (pb)	σ_{Radion} (pb)
$^{40}_{18}Ar$	$\gamma\gamma$	6.433×10^{-4}	1.346×10^{-4}	3.024×10^{-5}
$^{40}_{18}Ar$	$b\bar{b}$	2.682×10^{-1}	1.036×10^{-1}	9.252×10^{-3}
$^{40}_{18}Ar$	gg	2.268×10^{1}	2.874×10^{-3}	1.334×10^{-1}

TABLE V. Cross Section in pb for the process $\gamma\gamma \to$ Final State with $m_H = m_R = 115$ GeV and $\Lambda_R = 4v = 984$ GeV ≈ 1 TeV in heavy ion collisions at LHC with the refined set of cuts of Equations (11) and (14). $\sigma_{Background}$ stands for the SM background without Higgs and/or Radion diagrams, σ_{Higgs} stands for the contribution $\gamma\gamma \to H \to$ Final State and σ_{Radion} stands for the contribution $\gamma\gamma \to R \to$ Final State.

Ion considered	Final State	Integrated Luminosity (pb^{-1})	Years
$^{40}_{18}Ar$	$\gamma\gamma$	1.649×10^{5}	2.618×10^{5}
$^{40}_{18}Ar$	$b\bar{b}$	1.331×10^{2}	2.112×10^{2}
$^{40}_{18}Ar$	gg	1.055×10^{7}	1.675×10^{7}
$^{40}_{20}Ca$	$\gamma\gamma$	1.082×10^{5}	1.804×10^{4}
$^{40}_{20}Ca$	$b\bar{b}$	8.731×10^{1}	1.455×10^{1}
$^{40}_{20}Ca$	gg	6.922×10^{6}	1.154×10^{6}

TABLE VI. Total Integrated Luminosity needed for a 95% C.L. Higgs signal for the process $\gamma\gamma \to$ Final State with $m_H = 115$ GeV in heavy ion collisions at LHC with the refined set of cuts of Equations (11) and (14). It is also presented the number of years needed for a 95% C.L. Higgs signal considering a luminosity of $0.63(6)pb^{-1}$ $year^{-1}$ for the Ar-Ar (Ca-Ca) mode as discussed in the text.

Ion considered	Final State	Integrated Luminosity (pb^{-1})	Years
$^{40}_{18}\mathrm{Ar}$	$\gamma\gamma$	1.143×10^{5}	1.814×10^{5}
$^{40}_{18}\mathrm{Ar}$	$b\bar{b}$	1.149×10^{2}	1.824×10^{2}
$^{40}_{18}\mathrm{Ar}$	gg	4.720×10^{3}	7.492×10^{3}
$^{40}_{20}\mathrm{Ca}$	$\gamma\gamma$	7.496×10^{4}	1.249×10^{4}
$^{40}_{20}\mathrm{Ca}$	$b\bar{b}$	7.541×10^{1}	1.257×10^{1}
$^{40}_{20}\mathrm{Ca}$	gg	3.097×10^{3}	5.161×10^{2}

TABLE VII. Total Integrated Luminosity needed for a 95% C.L. Higgs plus Radion signal for the process $\gamma\gamma \to$ Final State with $m_H = m_R = 115$ GeV and $\Lambda_R = 4v = 984$ GeV ≈ 1 TeV in heavy ion collisions at LHC with the refined set of cuts of Equations (11) and (14). It is also presented the number of years needed for a 95% C.L. Higgs plus Radion signal considering a luminosity of $0.63(6)\mathrm{pb}^{-1}$ year^{-1} for the Ar-Ar (Ca-Ca) mode as discussed in the text.

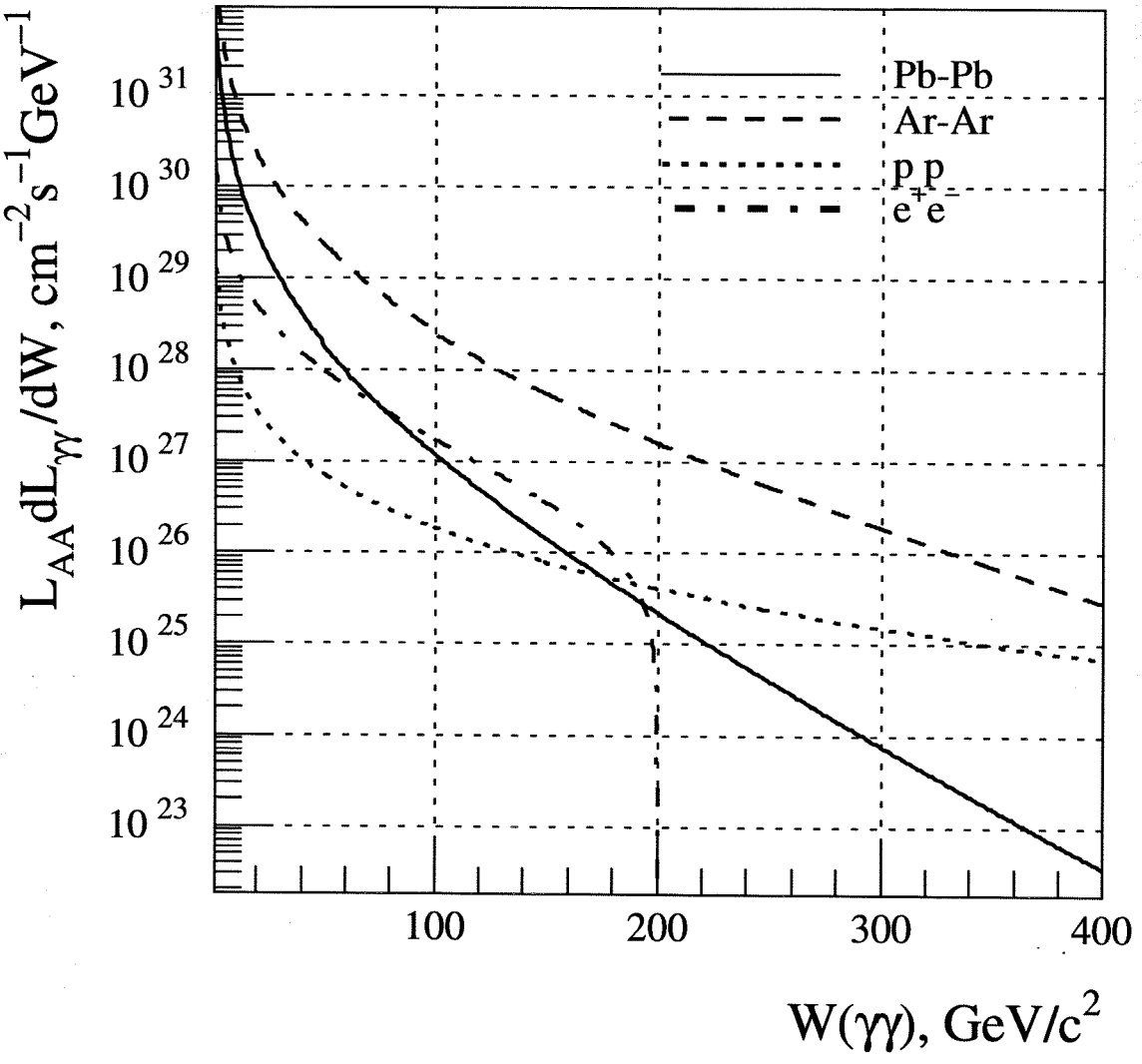

FIG. 1. Effective $\gamma\gamma$ luminosity at LHC for different ion species and protons as well as the e^+e^- collider LEPII in terms of the invariant mass of the pair of photons $W(\gamma\gamma)$.

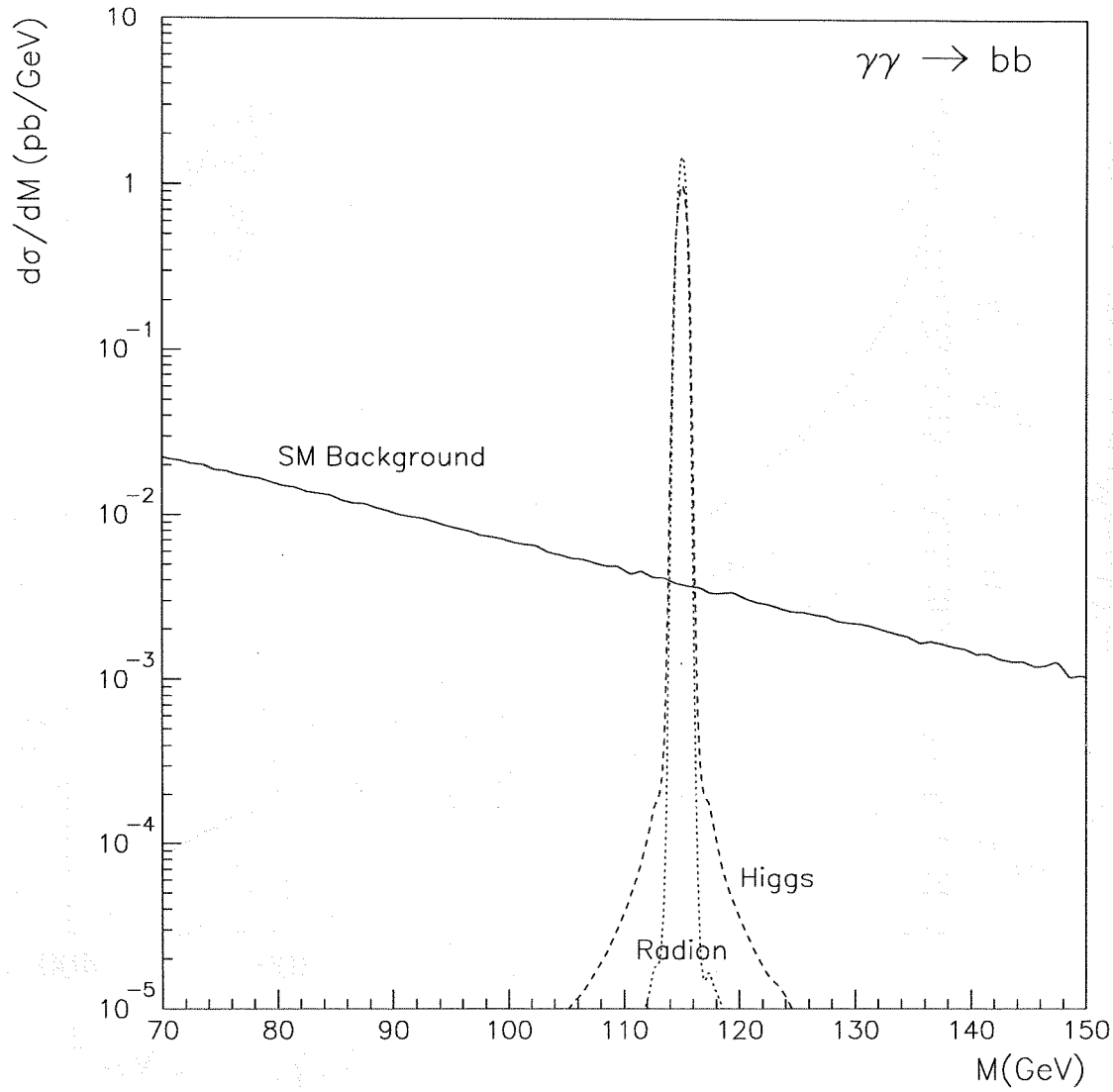

FIG. 2. Normalized invariant mass distribution of the $b\bar{b}$ pair with a Higgs mass and a Radion mass equal to 115 GeV and $\lambda_R = 4v \approx 1$ TeV. The full line corresponds to the SM background discussed in the text while the dashed (dotted) line corresponds to the Higgs (Radion) contribution.

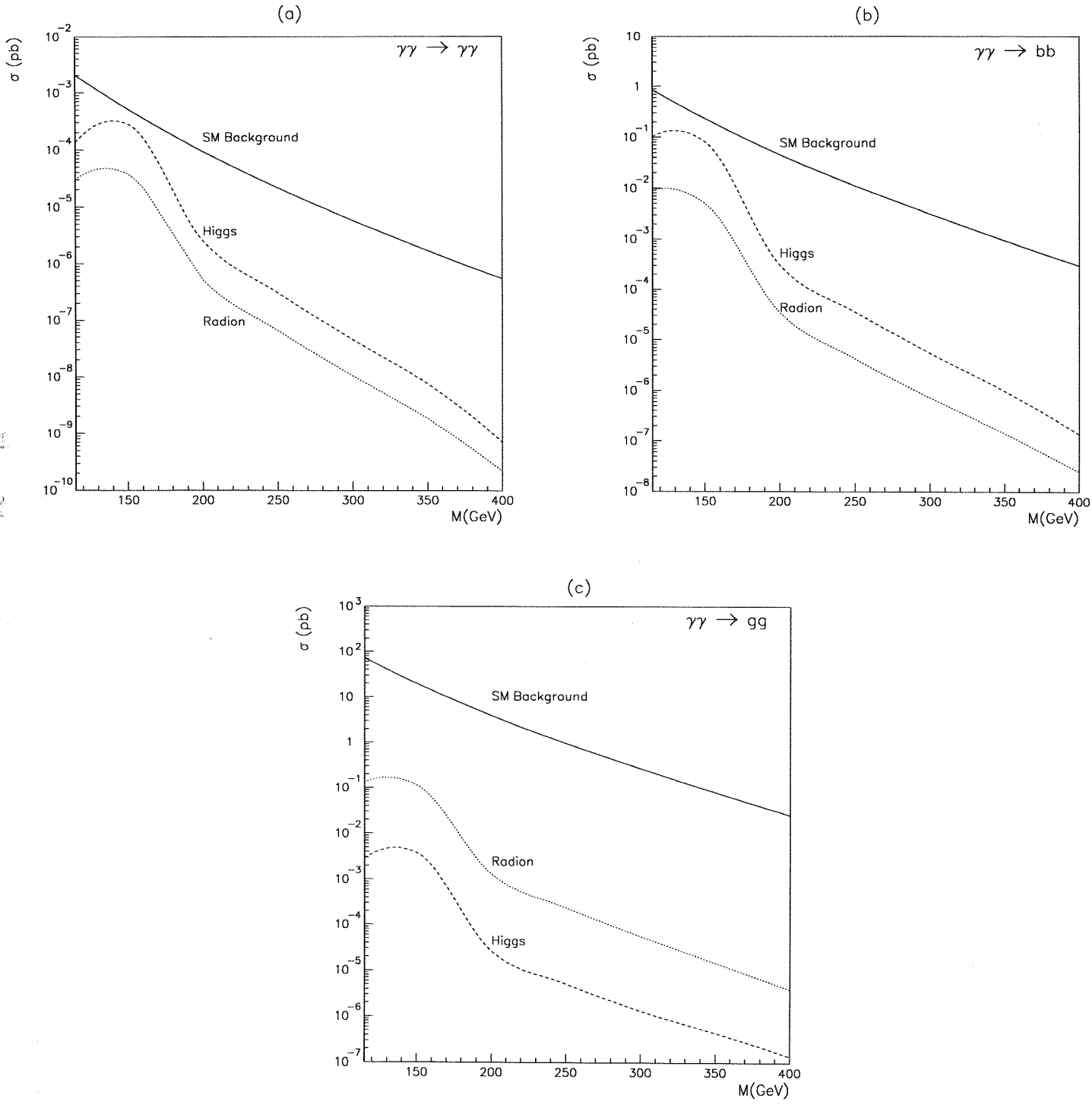

FIG. 3. Cross sections for the processes (a) $\gamma\gamma \to \gamma\gamma$, (b) $\gamma\gamma \to b\bar{b}$, and (c) $\gamma\gamma \to gg$, for $\lambda_R = 4v \approx 1$ TeV, considering events whose invariant masses fall in bins of size of 30 GeV around the mass M, as in Equation (12). The full line corresponds to the SM background discussed in the text while the dashed (dotted) line corresponds to the Higgs (Radion) contribution.

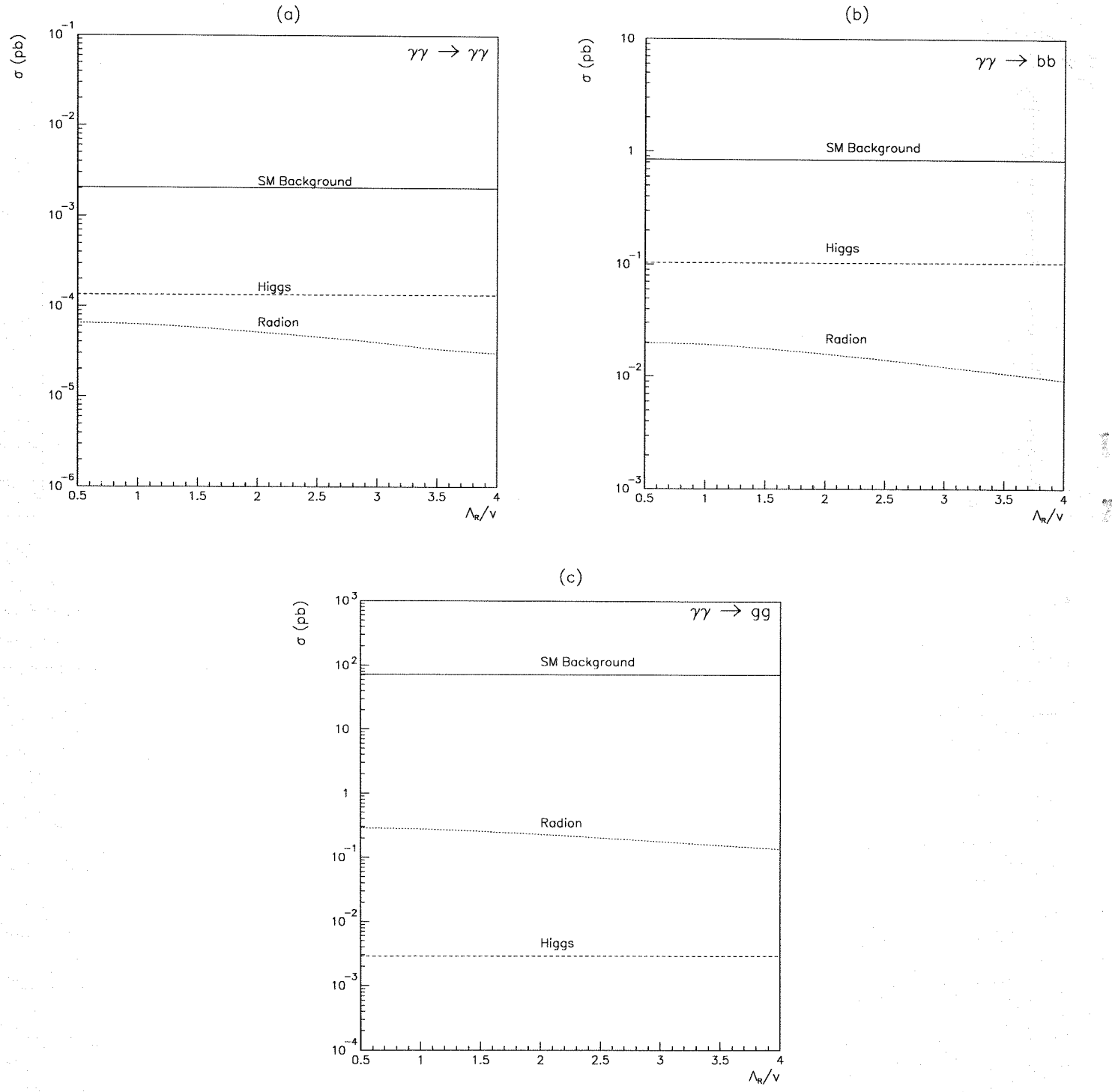

FIG. 4. Cross sections for the processes (a) $\gamma\gamma \to \gamma\gamma$, (b) $\gamma\gamma \to b\bar{b}$, and (c) $\gamma\gamma \to gg$ in terms of the ratio of the vev's of the Radion (Λ_R) and the Higgs (v) fields. The mass of the Higgs and/or Radion is equal to 115 GeV and the set of cuts given by Equations (11) and (12) was applied. The full line corresponds to the SM background discussed in the text while the dashed (dotted) line corresponds to the Higgs (Radion) contribution.

UNIVERSIDADE DE SÃO PAULO
Instituto de Física
Cidade Universitária
Caixa Postal 66.318
05315-970 - São Paulo - Brasil